Pis'ma v ZhETF, vol. 102, iss. 10, pp. 732 – 738

Complex singularities of fluid velocity autocorrelation function[1)]

N. M. Chtchelkatchev[+ 2)], *R. E. Ryltsev*[+*×]

[+] *Landau Institute for Theoretical Physics of the RAS, 142432 Chernogolovka, Russia*

[*] *Institute of Metallurgy UB of the RAS, 620016 Ekaterinburg, Russia*

[×] *Ural Federal University, 620002 Ekaterinburg, Russia*

Submitted 18 September 2015

Resubmitted 5 October 2015

There are intensive debates regarding the nature of supercritical fluids: if their evolution from liquid-like to gas-like behavior is a continuous multistage process or there is a sharp well defined crossover. Velocity autocorrelation function Z is the established detector of evolution of fluid particles dynamics. Usually, complex singularities of correlation functions give more information. So we investigate Z in complex plane of frequencies using numerical analytical continuation. We have found that naive picture with few isolated poles fails describing $Z(\omega)$ of one-component Lennard–Jones (LJ) fluid. Instead we see the singularity manifold forming branch cuts extending approximately parallel to the real frequency axis. That suggests LJ velocity autocorrelation function is a multiple-valued function of complex frequency. The branch cuts are separated from the real axis by the well-defined "gap" whose width corresponds to an important time scale of a fluid characterizing crossover of system dynamics from kinetic to hydrodynamic regime. Our working hypothesis is that the branch cut origin is related to competition between one-particle dynamics and hydrodynamics. The observed analytical structure of Z is very stable under changes of temperature; it survives at temperatures which are by the two orders of magnitude higher than the critical one.

DOI: 10.7868/S0370274X15220038

Introduction. There are intensive debates regarding the nature of supercritical fluids: if their evolution from liquid-like to gas-like state is characterised by a single sharp crossover [1, 2] or it is continuous multistage process [3–6] (that agrees with standard textbook results). Velocity autocorrelation function Z is the established detector of evolution of fluid particles dynamics [7]; it provides important information about correlation times in the system. As a rule, using the results of numerical simulations, the only real-frequency spectrum $\tilde{Z}(\omega)$ is studied. However, interesting fitches of $\tilde{Z}(\omega)$ should be hidden in the complex ω plane. So we investigate Z of simple fluid at complex frequencies using numerical analytical continuation. We show how the singularities of $\tilde{Z}(\omega)$ evolve with temperature and relate their location with correlation times of the fluid.

Velocity autocorrelation function is the correlator of particle velocity, $Z(t) = \langle \mathbf{v}(t) \cdot \mathbf{v}(0) \rangle$, where averaging is performed over particle trajectories. The Fourier transform of $Z(t)$ presents the density of vibrational states and may be written in the form [7]:

$$\tilde{Z}(\omega) = \frac{A}{-i\omega + \tilde{M}(\omega)}, \qquad (1)$$

where A is a constant and $\tilde{M}(\omega)$ is the so-called memory function which plays the role of friction coefficient that is non-local in time. Here tilde above Z means that we put $Z(t < 0) = 0$.

There is some analogy between (1) and Greens functions in quantum theory of strongly correlated electron systems. For electrons in normal metal (retarded), Greens function in the Fourier space can be written as $G^r(\omega) = 1/(\omega - \Sigma^r)$, where Σ^r is the self energy. Poles of the Greens function give spectrum and lifetime of quasiparticle excitations [8]. Greens functions in superconductors are more complicated: their complex singularities may include branch cuts related to the formation of the superconducting gap.

Long ago it was realised that poles of $\tilde{Z}(\omega)$ may have important physical interpretation. It was shown that temperature evolution of simple fluid $Z(t)$ can be qualitatively described by the exponential memory function $M(t) = M(0)\exp(-t/\tau)$ with the single relaxation time $\tau = T/D\omega_{\mathrm{E}}^2$, where T is temperature,

[1)] See Supplemental material for this paper on JETP Letters suite: www.jetpletters.ac.ru.

[2)] e-mail: rrylcev@mail.ru

D is the diffusion coefficient and $\omega_{\rm E}$ is the Einstein frequency (oscillation frequency of the particle in the effective potential formed by the surrounding particles), see Ref. [7] for review. Within this approximation $\tilde{M}(\omega) = \omega_{\rm E}^2/(-i\omega + 1/\tau)$ and so the time dependence of Z is simply determined by two poles of $\tilde{Z}(\omega)$. Then $Z(t)$ demonstrates damped oscillations with frequency and damping rate determined by the real and imaginary parts of the poles respectively. The model predicts bifurcation in density-temperature plane corresponding to the supercritical fluid states. The bifurcation occurs when the real part of the poles vanishes and so $Z(t)$ becomes monotonically decaying function of time. Even though the model qualitatively reproduces evolution of fluid $\tilde{Z}$ with temperature and pressure (density), but the quantitative accuracy of the approximations is rather low.

The memory function $\tilde{M}(\omega)$ can be formally written as infinite continued fraction of frequency, see Ref. [9] for review: $\tilde{M}(\omega) = \frac{m_1}{-i\omega + \frac{m_2}{-i\omega + \ldots}}$, where m_i, $i = 1, 2, \ldots$ are constants related to the frequency moments. The general problem is that one has to truncate somehow the continued fraction and so this approach fails describing hydrodynamic time scales, $t \gg \tau$, where $Z(t)$ shows the universal long-time tails governed by hydrodynamic fluctuations, see Refs. [7, 10, 5]. In liquid state, hydrodynamic tails are not very important (for three-dimensional system) but in the supercritical fluid state, that we also investigate here, they may provide up to 30 % of the diffusion coefficient (we remind that $D \propto \int_0^\infty Z(t)dt$).

Although no reliable analytical equation can be provided for Z, the very idea to investigate properties of supercritical fluid in complex singularities of $\tilde{Z}(\omega)$ is quite promising. In order to do it, we use molecular dynamic (MD) simulations to find $Z(t)$ and then use Pade-approximant method for analytical continuation.

We see the singularity manifold forming branch cuts extending approximately parallel to the real frequency axis. That suggests LJ velocity autocorrelation function is a multiple-valued function of complex frequency. The branch cuts are separated from the real axis by the well-defined gap whose width Δ_ω corresponds to some correlation time $\Delta t = 2\pi/\Delta_\omega$. We observe that $\Delta t \sim t_h$, where t_h corresponds to crossover of system dynamics from kinetic to hydrodynamic regime with $t^{-3/2}$ behavior of $Z(t)$. That suggests the origin of the branch cuts is an competition between one particles dynamics and hydrodynamics. The singularity structure is very stable under increase of the temperature; we have found its trace at temperatures even several orders of magnitude higher than the melting point. We draw Δt in Fig. 1. It follows that in whole range of studied temperatures, $\Delta t \approx 5t_{\rm E} = 2\pi/\omega_{\rm E}$.

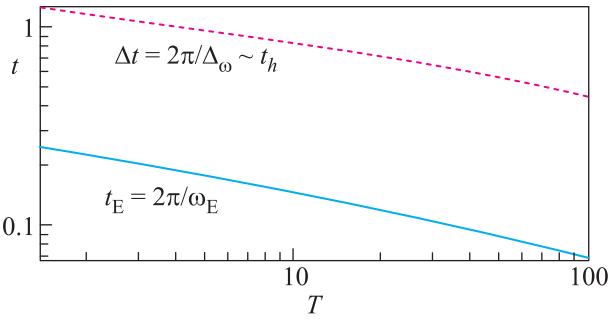

Fig. 1. (Color online) Correlation time $\Delta t = 2\pi/\Delta_\omega$ related to the branch cut width Δ_ω and the time scale related to Einstein frequency at density $\rho = 1$. We see that in whole range of studied temperatures, $\Delta t \approx 5t_{\rm E} = 2\pi/\omega_{\rm E}$

Below we briefly discuss the calculation procedure. We focus on simple LJ fluid. However this is only the first step: our method of complex-frequency analysis can be applied as well for binary and more complicated fluids.

Numerical analytical continuation. There are a number of approaches that allow doing numerical analytical continuation: the z-transform of DCF(t) (this is fast complex-ω Fourier transform) [11, 12], integration of Cauchy–Riemann equations or different methods of series reexpansion [13]. The most promising way is to built an approximation of $\tilde{Z}(\omega)$ at real ω by a meromorphic function and finally perform the analytical continuation of it. (In complex analysis, meromorphic function is a function that is holomorphic except a set of isolated points [14].) Usually this approximation is performed by the Pade approximant [15–17]. This method, for example, has been very effective for analytical continuation of the Greens function in superconductor theory from imaginary (Matsubara) frequencies to the real frequency domain [15]. Recently numerical analytical approximation allowed to uncover new physics in classical hydrodynamics of the Stokes waves [18].

Pade-approximants are the rational functions (ratio of two polinomials). They can be represented by a continued fraction. Typically the continued fraction expansion for a given function approximates the function much better than its series expansion. Here, we use "multipoint" algorithm [16] to build the Pade-approximant. Suppose we know function values $f(x_i) = u_i$ in the discrete set of points x_i where the

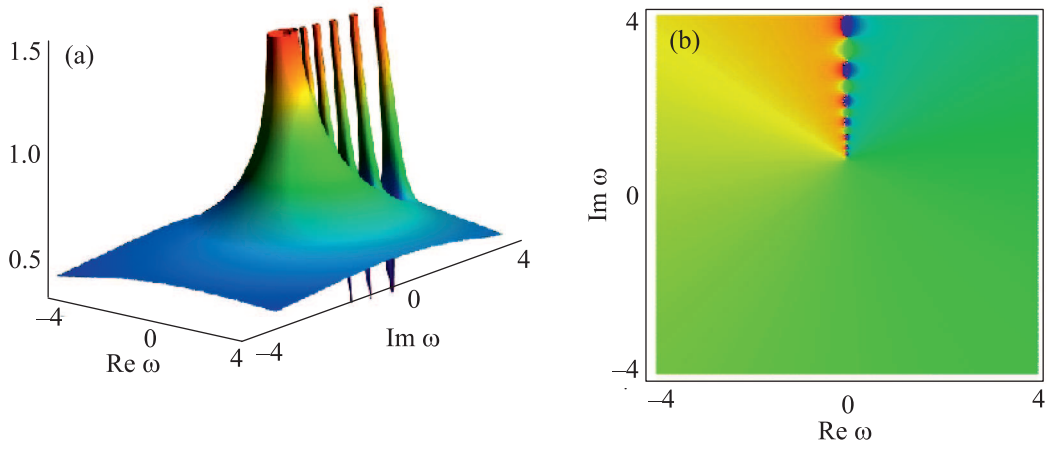

Fig. 2. (Color online) Analytical continuation of the square root function: (a) shows the absolute value while (b) is the argument. Array of peaks and dips in panel a represent the branch cut

"knots" x_i, $i = 1, 2, 3, \ldots, N$. Then the Pade approximant

$$C_N(x) = \cfrac{a_1}{\cfrac{a_2(x-x_1)}{\cfrac{a_3(x-x_2)}{\cfrac{a_4(x-x_3)}{\ldots a_N(x-x_{N-1})+1}+1}+1}+1}, \qquad (2)$$

where a_i we determine using the condition, $C_N(x_i) = u_i$, which is fulfilled if a_i satisfy the recursion relation

$$a_i = g_i(x_i), \quad g_1(x_i) = u_i, \quad i = 1, 2, 3, \ldots, N, \qquad (3)$$

$$g_p(x) = \frac{g_{p-1}(x_{p-1}) - g_{p-1}(x)}{(x - x_{p-1})\, g_{p-1}(x)}, \quad p \geq 2. \qquad (4)$$

Eq. (3) is the "boundary condition" for the recursive relation Eq. (4). For example, taking $x = x_{i_0}$ we get $g_1(x_i)$ from (3) and $g_j(x_{i_0})$, $j = 2, 3, \ldots, i$, from (4). The most accurate C_N corresponds to uniform distribution of "knots" x_i. Accuracy of the analytical continuation can be tested by permutations of x_i and/or by the random extraction of some part of the knots and permutation averaging.

Finally we take the function with the square root singularity to test and illustrate the Pade-approximation: $f_{\rm sqr}(\omega) = \sqrt{\omega - i}$. We build the Pade approximant using 300 uniformly distributed knots at real $\omega \in (-10, 10)$. Then we analytically continue the Pade polinomial (it is in fact complex even at real ω) to the complex ω-plane as shown in Figs. 2a and b. Array of peaks and dips in panel a represents the branch cut: this is typical for Pade approximation [16, 18]. More illustrating test examples of the Pade-approximation procedure are presented in Supplemental Material.

MD simulations. For MD simulations of $Z(t)$ we use the LJ pair potential model $U(r) = 4\varepsilon[(\sigma/r)^{12} - (\sigma/r)^6]$, where ε is the unit of energy and σ is the core diameter. In the remainder of this paper we use the dimensionless quantities: $\tilde{r} = r/\sigma$, $\tilde{U} = U/\varepsilon$, temperature $\tilde{T} = k_{\rm B}T/\varepsilon$, density $\tilde{\rho} \equiv N\sigma^3/V$, and time $\tilde{t} = t/(\sigma\sqrt{m/\varepsilon})$, where m and V are the molecular mass and system volume correspondingly. As we will only use these reduced variables, we omit below the tildes.

We have considered the system of $N = 128^3 \simeq \simeq 2.1 \cdot 10^6$ particles that were simulated under periodic boundary conditions in 3-dimensional cube, see Ref. [5]. We consider the system at fixed density $\rho = 1$ and different temperatures in the interval $T \in (1.4, 200)$. This range covers thermodynamic states from the liquid just above the melting line up to the supercritical fluid approaching the ideal gas limit [19, 20].

There are two ways how we can define $Z(t)$ at $t < 0$: 1) we can set $Z(t < 0) = 0$ or 2) we can demand $Z(t) \equiv Z(|t|)$. Fourier transform of $Z(t)$ in the first case we distinguish by tilde: $\tilde{Z}(\omega)$. It has singularities only at the lower half plane of complex ω [8]. The Fourier transform of $Z(t)$ in the second case we denote $Z(\omega)$, without tilde (same notations we use for Fourier transform of M). $Z(\omega)$ has complex singularities in the lower and upper ω half planes. Building the Pade approximant on top of $Z(\omega)$ we can take $x_i = \omega_i^2$ and focus on $\omega_i > 0$ since $Z(\omega)$ is real and even function of ω at real axis and there $Z(\omega) = {\rm Re}\,\tilde{Z}(\omega)$. We should also note that density of vibrational states corresponds to ${\rm Re}\,\tilde{Z}(\omega)$ at real ω, while ${\rm Im}\,\tilde{Z}(\omega)$ does not have much sense.

Fluid just above the melting line. We start our investigation from the case of $T = 1.4$ and $\rho = 1$: these parameters correspond to fluid just above the melting line. The results are shown in Figs. 3 and 4. $Z(t)$ obtained using MD simulations is shown in Fig. 3a and b represents $Z(\omega)$ obtained by Fourier transformation of

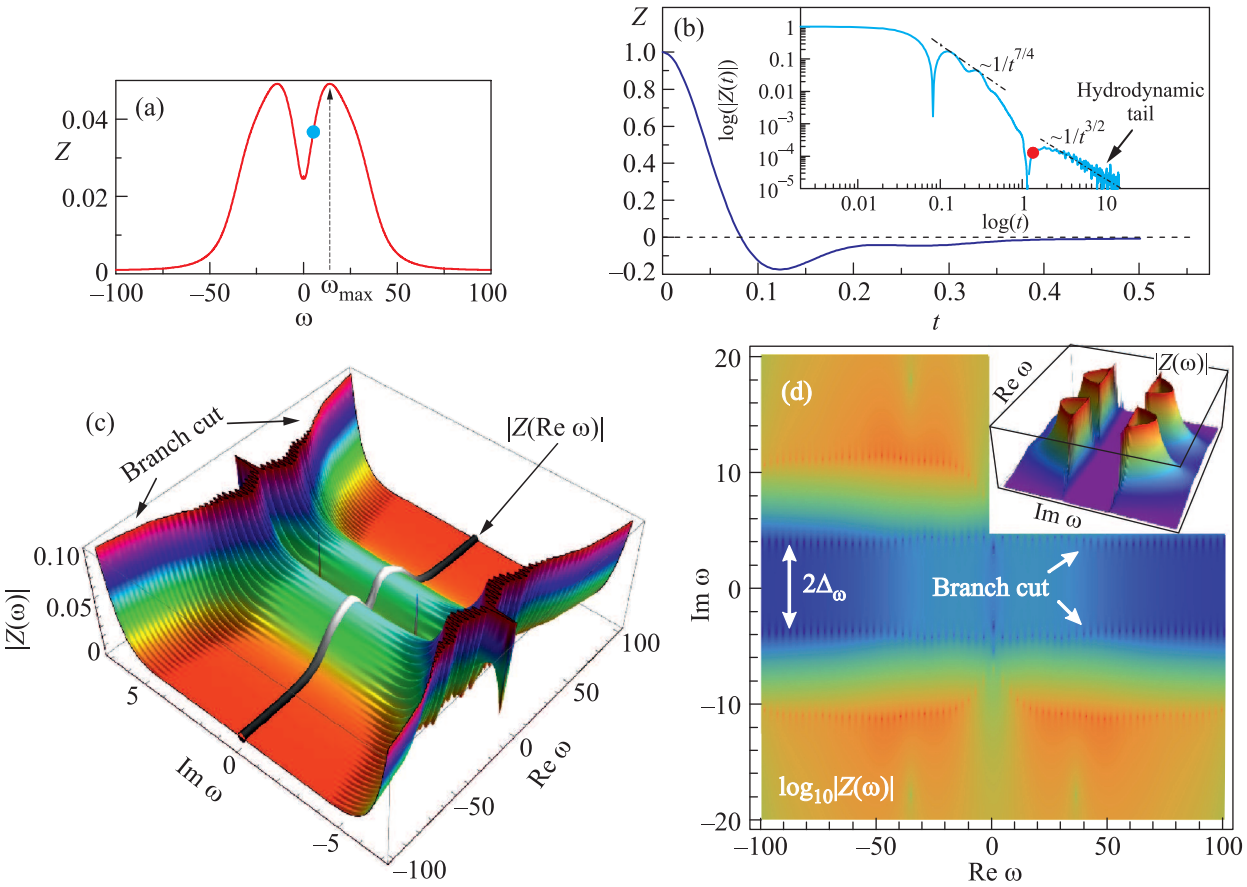

Fig. 3. (Color online) Velocity autocorrelation function in frequency (a) and in time (b) representation for $T = 1.4$ and $\rho = 1$: results of MD simulation. The inset in panel b shows long time tail of $Z(t)$; the red bullet points – the time scale $\Delta t = 2\pi/\Delta_\omega$, where Δ_ω (blue bullet in panel a) is the half-width of the branch cut. (c) – Analytical continuation of $Z(\omega)$ into complex ω-plane using multipoint Pade approximation. (d) – The density plot of $\log_{10}|Z(\omega)|$; insert schematically shows 3D behaviour of $|Z(\omega)|$ in the data range $(0, 10^5)$ for $\mathrm{Im}\,\omega \in (-40, 40)$ and $\mathrm{Re}\,\omega \in (-100, 100)$

$Z(t)$. At $t > 1$, $Z(t)$ becomes positive and as it should be in fluid [21], and at $t \gtrsim 5$ it demonstrates $t^{-3/2}$ asymptotic behaviour, see insert in Fig. 3b. We use this long time asymptotic to obtain high-quality Fourier transform of $Z(t)$. For that purpose, we perform extrapolation of $Z(t)$ to long times by $at^{-3/2}$ asymptotic with the appropriate value of a. (Of course, we have tested that this procedure does not change $Z(\omega)$ behavior and does not influence the properties of analytical continuation to complex ω-plane). As the result, we obtain smooth $Z(\omega)$ curve at all interesting values of ω (see Fig. 3b). The $Z(\omega)$ curve has the form typical to that for simple liquids [7]. In particular, it demonstrates pronounced maximum at $\omega = \omega_{\max}$.

Figs. 3c and d show analytical continuation of $Z(\omega)$ into complex ω-plane using multipoint Pade approximation built on top of 1400 uniformly distributed knot-points in $(0, 6.3\omega_{\max})$. Regular behaviour of $Z(\omega)$ for small imaginary frequencies ends abruptly by the "walls" of singularities constructed from poles (and zero nodes) of the Pade-approximant. Fig. 3d shows plot of $\ln|Z(\omega)|$ in the domain $\mathrm{Re}\,\omega$, $\mathrm{Im}\,\omega \in (-4.5\omega_{\max}, 4.5\omega_{\max})$. Such series of poles and zeros is the way the Pade approximation typically represents branch cuts of multi-valued functions (see Refs. [16, 18] and Fig. 2).

In the insert in Fig. 3b we show the long-time behaviour of $Z(t)$ in double logarithmic scales. The red bullet points the time scale $\Delta t = 2\pi/\Delta\omega$, where, we remind, $\Delta\omega$ is the characteristic scale approximately equal to the half-width of the gap between branch cuts. As follows, $\Delta t \sim t_h$, where t_h corresponds to crossover of system dynamics from kinetic to hydrodynamic regime.

Hydrodynamic singularity: additional branch cut at $\omega \to 0$. At timescales much larger than inverse Einstein frequency, Z is positive and it has the following asymptotic behaviour: $Z(t) \sim t^{-3/2}$ [7, 5] that results in singular terms in $Z(\omega \to 0) \sim \mathrm{const} - \sqrt{|\omega|}$ at real frequency axis, see Fig. 4a for illustration. This nonana-

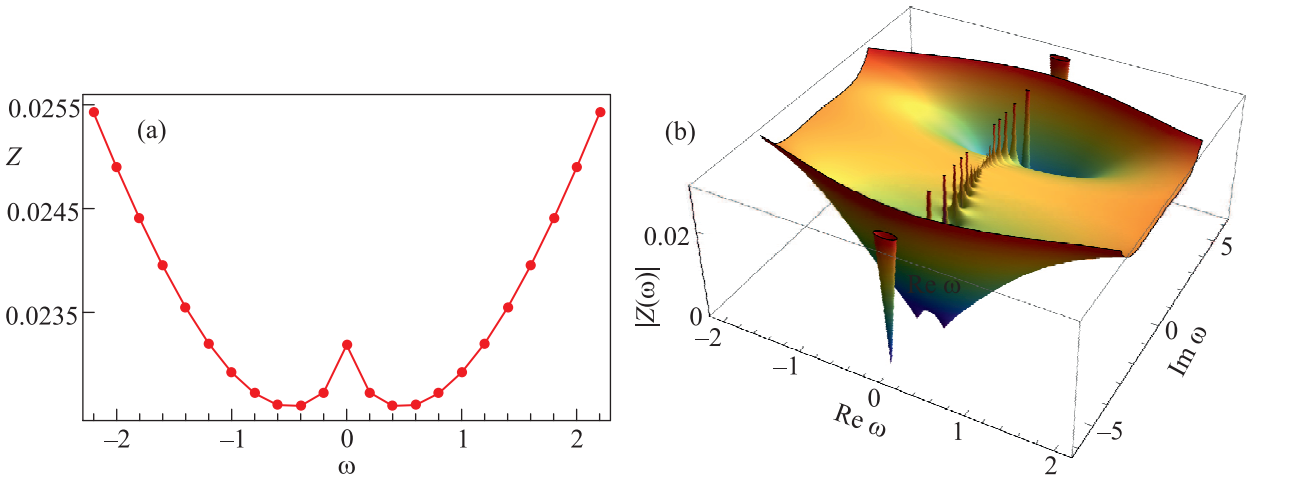

Fig. 4. (Color online) Hydrodynamic tales of $Z(t) \sim t^{-3/2}$ generate additional singular terms in $Z(\omega \to 0) \sim \text{const} - \sqrt{|\omega|}$ at real frequency axis (a). This nonanalyticity at $\omega = 0$ produces the sequence of poles and zero-knots located at the line $\text{Re}\,\omega = 0$ (b). This singularity sequence corresponds to the additional branch cut

lyticity at $\omega = 0$ should produce additional branch cut. We do see it in Fig. 4b where $Z(\omega)$ is shown. Preparing Fig. 4b we have used the same Pade approximant as we have used working on Figs. 3c and d. Hydrodynamic branch cut is on the imaginary axis and so it lies transversely to the branch cut presented in the Figs. 3c and d. Note that for liquid near the melting line hydrodynamic singularity is located at only small vicinity of $\omega = 0$ (compare Figs. 3a and 4a). Thus the hydrodynamic branch cut is only detectable at small frequency scales (compare Figs. 3c and d and 4d).

From fluid to gas: evolution of $Z(\omega)$. Below we test how stable is the the branch cut in $Z(\omega)$ when we increase the temperature of the fluid far above the melting line. It follows that the branch cut is very stable to temperature.

For density $\rho = 1$ the temperature $T = 40$ is characteristic temperature when fluid local structure vanishes, see Ref. [4]. However the branch cut in $Z(\omega)$ is still well observable, see Fig. 5.

Insert in Fig. 5b shows $Z(t)$ in double logarithmic scale. Dash-dotted line there sketches the hydrodynamic $\propto 1/t^{3/2}$-tail. The red bullet shows Δt. It follows that again $\Delta t \sim t_h$.

For density $\rho = 1$ and temperature $T = 200$ we have the slightly nonideal gas. However even at such high temperatures there is a branch cut, very small one, as follows from Fig. 6. Insert in Fig. 6b shows $Z(t)$ in double logarithmic scale, where the dash-dotted line sketches $\propto 1/t^{3/2}$-tail. The red bullet we again put at $t = \Delta t$. The relation $\Delta t \sim t_h$ is valid in that case too.

Except small branch cuts, Figs. 6c and d reveal two isolated poles located on the imaginary axis. The appearance of such poles at hight temperatures shows that the dynamics of the system is near to that for the ideal gas. Indeed the simplest low-density-limit exponential relation for $Z(t)$ obtaining from either the Enskog approximation or the Brownian one has the same analytical structure with two pure imaginary poles [7].

We did not discuss in detail the branch cut at the intermediate temperatures between $T = 1.4$ and 200 and other densities. At the intermediate temperatures we see monotonic change of the branch cut structure of VAF, see Fig. 1. More illustrations we leave for the forthcoming paper.

In order to check stability of our results under changes of system size, we have performed test simulations of the system of $N = 5 \cdot 10^8$ particles. The results obtained are qualitatively the same as those for $N = 2 \cdot 10^6$ particles. That suggests our main conclusions are stable to finite-size effects.

Conclusions. Singularities of dynamic correlation functions in complex-frequency plane usually correspond to the collective or localized modes. We have found that, instead of few number of isolated poles, VAF of LJ particle system in complex plane shows the singularity manifold forming branch cuts that suggests it is a multiple-valued function of complex frequency. The branch cuts are separated from the real axes by the well-defined "gap". The branch cuts are quite stable with the respect to temperature and density variation. We have found the trace of the singularity gap at temperatures several orders of magnitude higher than the melting temperature. Our working hypothesis is that the branch cut origin is related to the interference of short-time one-particle kinetics and long-time collective

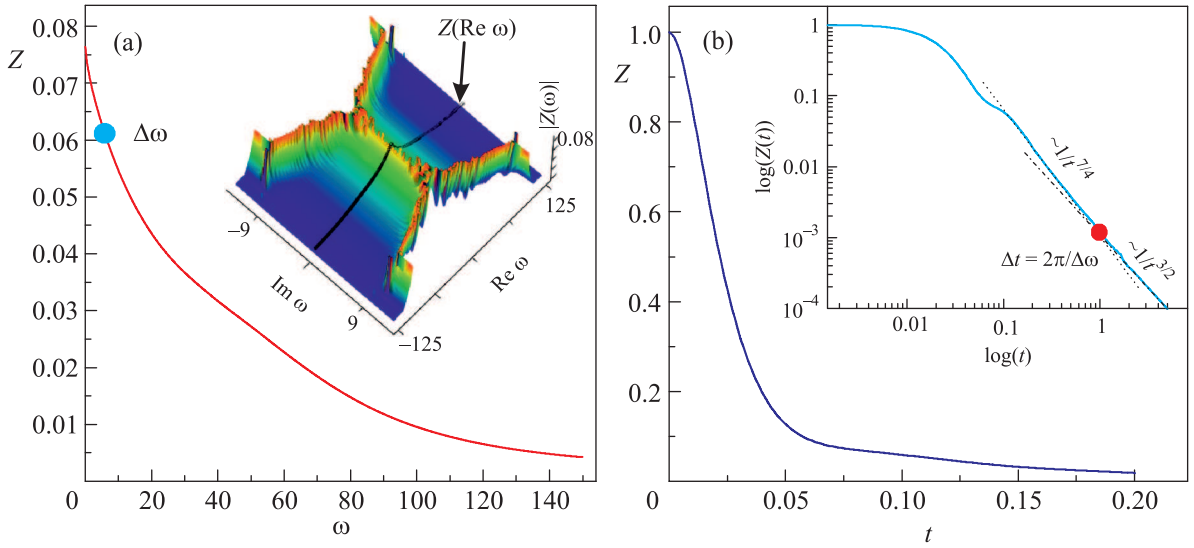

Fig. 5. (Color online) VAF at real frequency axis (a) and in time representation (b) for $T = 40$ and $\rho = 1$: results of MD simulation. Insert in panel a shows $|Z(\omega)|$. Insert in panel b shows $Z(t)$ in double logarithmic scale

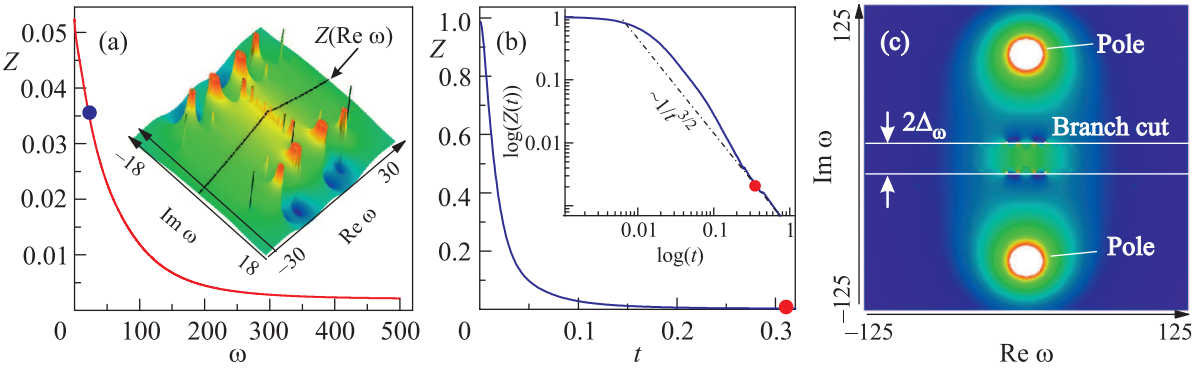

Fig. 6. (Color online) $Z(\mathrm{Re}\,\omega)$ (a) and $Z(t)$ (b) for $T = 200$ and $\rho = 1$: results of MD simulation. Graph c and insert in panel a show $|Z(\omega)|$ in complex ω-plane

motion (hydrodynamics). We suggest that numerical analytical continuation is a new effective tool that allows understanding hidden properties of fluids and soft matter systems. We show that, during the evolution of the system from liquid to gas states, the branch cut picture evolves continuously.

This work was supported by Russian Scientific Foundation (grant # RSF 14-12-01185).

1. D. Bolmatov, M. Zhernenkov, D. Zavyalov, S. Stoupin, Y. Q. Cai, and A. Cunsolo, J. Phys. Chem. Lett. **6**(15), 3048 (2015).
2. V. V. Brazhkin, Y. D. Fomin, A. G. Lyapin, V. N. Ryzhov, E. N. Tsiok, and K. Trachenko, Phys. Rev. Lett. **111**, 145901 (2013).
3. T. Bryk, Phys. Rev. E **91**, 036101 (2015).
4. R. E. Ryltsev and N. M. Chtchelkatchev, Phys. Rev. E **88**, 052101 (2013).
5. R. E. Ryltsev and N. M. Chtchelkatchev, J. Chem. Phys. **141**(12), 124509 (2014).
6. G. Ruppeiner, P. Mausbach, and Helge-Otmar May, Phys. Lett. A **379**, 646 (2015).
7. J.-P. Hansen and I. R. McDonald, *Theory of Simple Liquids*, Academic Press (2013).
8. A. A. Abrikosov, L. P. Gorkov, and I. E. Dzyaloshinski, *Methods of Quantum Field Theory in Statistical Physics*, Courier Corporation (1975).
9. A. Mokshin, Theor. Math. Phys. **183**, 449 (2015).
10. M. H. Ernst, E. H. Hauge, and J. M. J. van Leeuwen, Phys. Rev. Lett. **25**, 1254 (1970).
11. G. R. Kneller and K. Hinsen, J. Chem. Phys. **115**(24), 11097 (2001).
12. S. H. Krishnan and K. G. Ayappa, J. Chem. Phys. **118**, 690 (2003).

13. L. Reichel, Constructive Approximation **2**, 23 (1986).
14. M. Lavrentiev and V. Shabat, *Functions of Complex Variables Theory and Methods*, Nauka Publishers, M. (1973).
15. H. Vidberg and J. Serene, J. Low Temp. Phys. **29**, 179 (1977).
16. G. A. Baker and P. R. Graves-Morris, *Padé Approximants*, Cambridge University Press (1996), v. 59.
17. H. Yamada and K. Ikeda, Eur. Phys. J. B **87**, 1 (2014).
18. S. Dyachenko, P. Lushnikov, and A. Korotkevich, JETP Lett. **98**, 675 (2014).
19. B. Smit, J. Chem. Phys. **96**, 8639 (1992).
20. S.-T. Lin, M. Blanco, and W. A. Goddard, J. Chem. Phys. **119**, 11792 (2003).
21. S. R. Williams, G. Bryant, I. K. Snook, and W. van Megen, Phys. Rev. Lett. **96**, 087801 (2006).